OSCILLATION EFFECTS IN SEMIMETALLIC $Bi_{1-x}Sb_x$ *ALLOYS UNDER PRESSURE*

N. B. BRANDT and S. M. CHUDINOV

Moscow State University

Submitted May 26, 1970

Zh. Eksp. Teor. Fiz. 59, 1494–1508 (November, 1970)

We investigate the combined action of hydrostatic pressures p up to 18 kbar and of strong magnetic fields H up to 74 kOe on the energy spectrum of $Bi_{1-x}Sb_x$ alloys with Sb concentrations from $x = 0.02$ to $x = 0.055$ at temperatures 1.9–4.2°K. A monotonic decrease of the extremal electron and hole sections of the Fermi surface and a changeover into the semiconducting state were observed for the alloys with $x < 0.04$ at a certain pressure $p = p_{cr}$ that depends on the Sb concentration. It is shown that for these alloys, the decrease of the overlap energy ϵ_{0v} under pressure is a result of the growth of the energy gap ϵ_g at the point L, at a rate $\sim 10 \times 10^{-6}$ eV/bar, and also the result of the lowering of the top of the valence band at T (relative to the center of the gap ϵ_g), at a rate $\sim 0.8 \times 10^{-6}$ eV/bar. It was observed that in alloys with $x > 0.04$, hydrostatic compression first increases the electron and hole extremal sections S^e and S^h, which pass through a maximum at a certain $p = p_m$, after which they decrease and vanish at $p = p_{cr}$. It is shown that the irregular character of the dependence of the sections on the pressure is connected with a qualitatively new character (relative to alloys with $x < 0.04$) of the motion of the energy terms: when $x > 0.04$ the gap ϵ_g decreases under pressure to an anomalously low value at $p = p_m$, at a rate $\sim 2.4 \times 10^{-6}$ eV/bar, after which, following the inversion of the terms L_a and L_s, it again increases at a rate $\sim 1.0 \times 10^{-6}$ eV/bar. The motion of the top of the valence band at T for alloys with $x > 0.04$ remains the same as for alloys with $x < 0.04$.

INTRODUCTION

AN investigation of the influence exerted on the spectrum of Bi by the combined action of an Sb impurity, a strong magnetic field, and hydrostatic compression is of interest from various points of view. Each of these parameters changes the spectrum of Bi in a definite manner, causing a shift of the end points of the energy bands and of the energy extrema in the bands. The simultaneous action of these parameters not only uncovers additional possibilities for the rearrangement of the spectrum of Bi in practically any direction and for constructing a substance with an unusual structure and unusual properties, but also makes it possible to obtain new information concerning the initial structure of the spectrum and the law governing the carrier dispersion in Bi and in $Bi_{1-x}Sb_x$ alloys.

In addition, the decrease of the energy intervals in the spectrum under the influence of the Sb impurity and of the pressure greatly expands the possibilities for observing and investigating the electronic phase transitions of I. Lifshitz[1] and the electronic phase transitions in the magnetic field[2], at which the properties of substances are qualitatively altered.

We report in this paper the results of an investigation of the Shubnikov–de Haas oscillations and of the non-oscillating component of the magnetoresistance $\rho(H)$ of $Bi_{1-x}Sb_x$ alloys at pressures up to 18 kbar, magnetic fields up to 74 kOe, and Sb concentrations from $x = 0.02$ to $x = 0.055$. We obtain the dependence of the sections of the electron and hole parts of the Fermi surface, and also of the cyclotron masses on the pressure and on the Sb concentration. An attempt is made to relate the characteristics of the curve of longitudinal magnetoresistance with the parameters of the spectrum of the alloys.

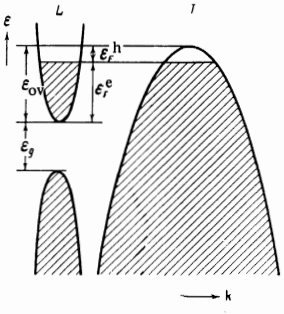

FIG. 1. Schematic energy spectrum of $Bi_{1-x}Sb_x$ alloys with Sb concentrations $x < 0.06$ (5) (k–wave vector).

A schematic spectrum of the $Bi_{1-x}Sb_x$ alloys with Sb concentrations smaller than 0.06 (5) is shown in Fig. 1. Here ϵ_F^e, ϵ_F^h, ϵ_{0v}, and ϵ_g denote respectively the Fermi energies of the electrons and the holes, the overlap energy, and the energy gap at L.

1. MEASUREMENT PROCEDURE. SAMPLES

Pressures up to 18 kbar were produced in the modernized bomb described in[3]. The pressure was determined from the temperature shift of the superconducting transition of tin, registered by an electronic method. The media transmitting the pressure were mixtures of dehydrated kerosene or pentane with transformer oil. The latter mixture made it possible to increase greatly the hydrostatic character of the pressure.

Magnetic fields up to 74 kOe were produced with a superconducting solenoid having a working-aperture diameter 26 mm and a winding length 80 mm. The voltage from the potential contacts of the samples was amplified with an F116/1 photoelectric amplifier and plotted with an x-y recorder with slow application of the magnetic field H. To separate the oscillating part

of the longitudinal magnetoresistance in the individual sections of the $\rho(H)$ curves, we used linear compensation of the non-oscillating part. To this end, a voltage proportional to H but of opposite polarity was applied to the input of the photoamplifier in series with the voltage from the sample.

The oscillations of the magnetoresistance were also investigated in a transverse magnetic field with the aid of a modulation procedure[4]. Compensation of the non-oscillating part of the derivative of the magnetoresistance $\partial\rho/\partial H$ was likewise used at certin values of the magnetic field, making it possible to improve greatly the sensitivity of the method.

Single-crystal ingots of high-grade $Bi_{1-x}Sb_x$ alloys were obtained from the laboratory of Professor G. A. Ivanov at the Leningrad State Pedagogical Institute.

The samples, in the form of rectangular parallelepipeds 2—2.5 mm long and 7.0×0.8 mm in cross section were cut from the single crystals by the electric-spark procedure. The Sb concentration in the alloys was determined accurate to 0.05 at.% by the method of radioactivation analysis. Prior to the mounting, the samples were etched in a mixture 50% C_2H_5OH and 50% HNO_3. The current electrodes were soldered to the entire end surface, and the potential electrodes of 40 μ diameter were welded with the aid of an electric-spark tacking device[5].

To accelerate the measurements, two samples were placed simultaneously in the working channel of the bomb. The samples were placed parallel or perpendicular to each other. The accuracy with which the magnetic field was oriented relative to the faces of the samples was $\pm 2^\circ$. For each pair of samples we verified the reproducibility of the results while decreasing the pressure.

2. MEASUREMENT RESULTS

At an Sb concentration $x \sim 0.04$, $Bi_{1-x}Sb_x$ alloys experience a band inversion at the point L, at which the terms L_S and L_a, which served at $x < 0.04$ respectively as the bottom of the conduction band and the top of the valence band at L (Fig. 1), approach each other to an anomalously short distance at $x \sim 0.04$, exchange places, and move apart at $x > 0.04$ (see, for example,[6-8]).

Connected with the inversion of the terms L_a and L_S are differences in the behavior under pressure of

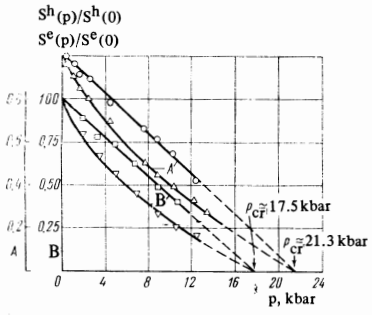

FIG. 2. Relative change, under pressure, of the extremal electron section (A, Δ) and hole section (A, ○) of a sample of $Bi_{0.98}Sb_{0.02}$ (**H** ∥ C_2), and the same (B, ▽ and B, □) for a sample of $Bi_{0.9725}$, $Sb_{0.0275}$ (**H** ∥ C_2); C_2 is the binary axis.

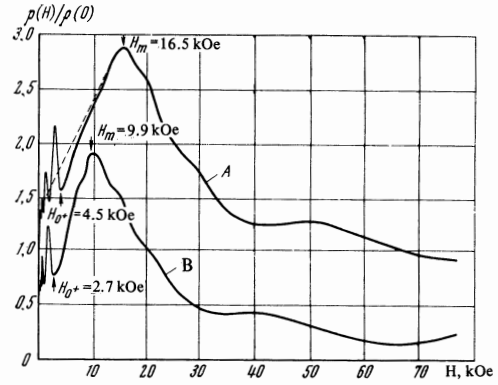

FIG. 3. General form of the plot of the magnetoresistance curves for the alloy $Bi_{0.954}Sm_{0.046}$ at **i** ∥ **H** ∥ C_2: A—p = 1 bar, B—p = 5.8 kbar (the curve B is shifted by an arbitrary amount along the ordinate axis.

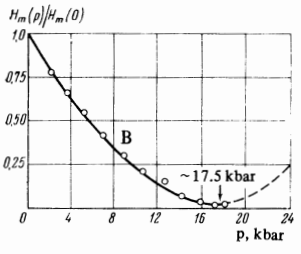

FIG. 4

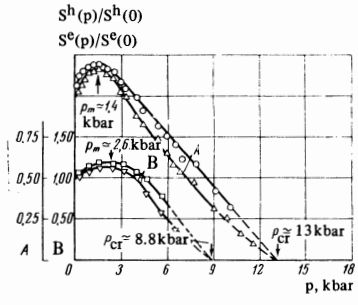

FIG. 5

FIG. 4. Relative change, under pressure, of the position of the maximum on the $\rho(H)$ curve (Fig. 3) at **i** ∥ **H** ∥ C_2 for a $Bi_{0.9725}Sb_{0.0275}$ sample at T = 4.2°K.

FIG. 5. Relative change, under pressure, of the extremal sections of the electrons (A, Δ) and holes (A, ○) of the sample $Bi_{0.954}Sb_{0.046}$ (**H** ∥ C_3, C_3—trigonal axis), and of the electrons (B, ▽) and holes (B, □) of the sample $Bi_{0.945}Sb_{0.055}$ (**H** ∥ C_2).

$Bi_{1-x}Sb_x$ alloys lying to the left and to the right of the inversion point.

1. $Bi_{1-x}Sb_x$ Alloys with $x < 0.04$

A plot, typical for these alloys, of the electron and hole extremal Fermi surfaces S^e and S^h against the pressure is shown in Fig. 2. Each of the sections, and consequently also the overlap energy, decreases monotonically under pressure. The $S^e(p)$ and $S^h(p)$ curves are similar to the analogous plots obtained for pure Bi in[9-11].

With increasing pressure, the amplitude of the oscillations decreases both as a result of the decrease of ϵ_{0V} and as a result of the increasing deviation of the pressure in the bomb from hydrostatic, something particularly noticeable when the kerosene-oil sample is used. We were unable to observe in practice any oscillations of the magnetoresistance in $Bi_{1-x}Sb_x$ samples with $x < 0.04$ starting with a pressure of ~ 14 kbar. As the pressure was being decreased from $p \sim 18$ kbar, the oscillations became noticeable again at $p < (12—14)$ kbar, and the period of the oscillations in terms of the reciprocal field (the magnitude of the period was inversely proportional to S) could be reproduced accurate to 5%. After complete removal of

the pressure, an irreversible decrease of the oscillation amplitude, by 20—30%, was observed. Extrapolation of the $S^e(p)$ and $S^h(p)$ curves to zero makes it possible to determine approximately the pressure p_{cr} at which the alloy goes over into the semiconducting state.

Typical curves of the magnetoresistance $\rho(H)$ ($i \parallel H \parallel C_2$; C_2—binary axis, i—current through the sample) at two values of the pressure are shown in Fig. 3. We see that the non-oscillating component of $\rho(H)$ first increases in the field, goes through a maximum at a certain $H = H_m$, and then decreases.

Investigations of $Bi_{1-x}Sb_x$ alloys carried out in pulsed magnetic fields at atmospheric pressure[12,13] have shown that $\rho(H)$ ($i \parallel H \parallel C_2$) is also described by a curve with a maximum, with H_m dependent on the Sb concentration and apparently indirectly connected with the alloy spectrum parameters.

In alloys with $x < 0.04$, the value of H_m decreases monotonically under pressure. In the region $p < p_{cr}$, the approximate equality $H_m(p)/H_m(0) \approx S^e(p)/S^e(0)$ is satisfied; this equality is noticeably violated only near $p \sim p_{cr}$ (see curves B on Figs. 2 and 4).

The correlation between the indicated quantities becomes even more clearly pronounced for alloys with $x > 0.04$.

2. $Bi_{1-x}Sb_x$ Alloys with $0.06(5) > x > 0.04$

In the Sb concentration region from 0.04 to 0.06 (5) we observed a nonmonotonic dependence of the electron and hole extremal sections S^e and S^h on the pressure. The sections first increase, pass through a maximum at $p = p_m$, and then decrease to zero at $p = p_{cr}$. The value of p_m increases with increasing Sb concentration. The relative changes of the cross sections under pressure for alloys with $x = 0.046$ and $x = 0.055$ are shown in Fig. 5.

For all the investigated alloys, in fields up to 74 kOe, the ultraquantum limit was reached for the electrons at L, and emergence of the Landau 0^+ level was observed. It was noted that when the cross section of the electron ellipsoid is changed under pressure with a given Sb concentration and for a given orientation of field H, S^e remains approximately proportional to the field H^e_{0+} corresponding to the emergence of the 0^+ level.

This circumstance was used to determine S^e for the alloys $Bi_{0.945}Sb_{0.055}$ and $Bi_{0.954}Sb_{0.046}$ at sufficiently small values of ϵ_{0v}, when the small number of the oscillations did not make it possible to determine their period reliably. The parts of curves A and B corresponding to this region are shown dashed in Fig. 5.

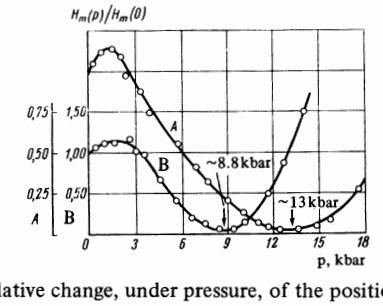

FIG. 6. Relative change, under pressure, of the position of the maximum on the $\rho(H)$ curve at $i \parallel H \parallel C_2$ for the samples $Bi_{0.954}Sb_{0.046}$ (A) and $Bi_{0.945}Sb_{0.055}$ (B).

The non-oscillating part of the $\rho(H)$ dependence ($i \parallel H \parallel C_2$) for alloys with $x > 0.04$, just as for alloys with $x < 0.04$, passes through a maximum at a certain $H = H_m$, which depends on the Sb concentration and on the pressure. So long as the overlap remains, one observes here, too, an approximate equality of $H_m(p)/H_m(0)$ and $S^e(p)/S^e(0)$; this equality is violated only in the region $p \sim p_{cr}$, where H_m reaches a minimum (at $p \approx p_{cr}$ we have $\partial H_m/\partial p = 0$), and the cross section S^e vanishes (curves A and B on Figs. 5 and 6).

Just as for alloys with $x < 0.04$, the value of H_m changes little with decreasing temperature when $p < p_{cr}$. In this region, the temperature variation of H_m is analogous to the variation in the fields corresponding to the minima and maxima of the oscillations.

After the overlap is lifted, H_m increases with pressure and reveals a strong dependence on the temperature. When the pressure is decreased, the maximum shifts appreciably towards larger magnetic fields. Such a behavior of H_m at $p > p_{cr}$ indicates that the maximum on the $\rho(H)$ curve in the superconducting state is determined by the thermal gap produced in the alloy under pressure.

3. Cyclotron Masses of Carriers

From the ratio of the magnetoresistance-amplitude oscillations at two temperatures, we calculated the cyclotron masses at the Fermi level. Calculation of the masses by the formulas of Adams and Holstein[14] is valid at a constant Dingle factor in the helium temperature region. By way of a control, the Dingle factor was calculated for each temperature from the dependence of the oscillation amplitude on the magnetic field.

The reduction of the data has shown that the hole cyclotron masses m^h for the $Bi_{1-x}Sb_x$ alloys are independent, within the limits of measurement accuracy, of the Sb concentration and of the pressure, and coincide with the corresponding masses for pure Bi. Thus, in a field parallel to the binary axis, the measured values of m^h lie in the interval $(0.185—0.22)\,m_0$, where m_0 is the mass of the free electron. The corresponding mass for pure Bi is $0.21\,m_0$[15,16]. This result is in good agreement with the universally accepted premise that the dispersion of the holes is close to quadratic.

The electron cyclotron masses m^e decrease appreciably with increasing Sb concentration. The dependence of m^e on x is shown in Fig. 7 (curve A). For comparison, the same figure shows the x-dependence of the electron cyclotron mass at the bottom of the band, m^e_0, obtained by Tichovolsky and Mavroides[7] from magneto-optical measurements (curve B). This curve shows the points calculated by the Lax-Golin method on the basis of the experimentally measured m^e and Se. For each Sb concentration, a weak decrease of m^e under pressure is observed. Figure 8 shows data on the pressure dependence of m^e for the alloy $Bi_{0.9725}Sb_{0.0275}$. The solid curve in this figure is the result of calculation by the Lax-Golin method (see the next section).

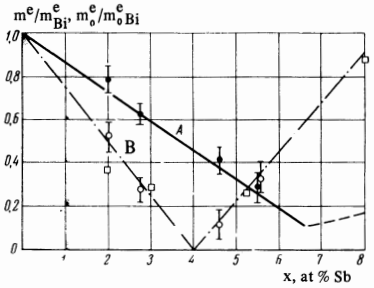

FIG. 7

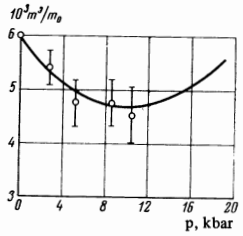

FIG. 8

FIG. 7. Ratio of electron cyclotron masses at the Fermi level (curve A) and at the bottom of the conduction band (curve B) to the corresponding masses for Bi vs the Sb concentration: ●—present data, □—data of [7], ○—result of calculation by formulas (3) and (5); solid curve—result of calculation by formula (6) on the basis of the data of the present article.

FIG. 8. Pressure dependence of the electron cyclotron mass for the sample $Bi_{0.9725}Sb_{0.0275}$ ($H \parallel C_2$); solid line—result of calculation by formula (6).

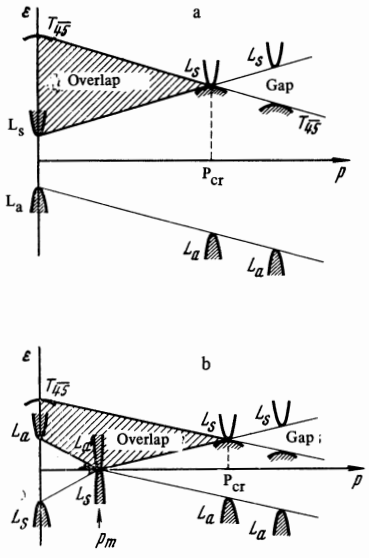

FIG. 9. Qualitative plot of the energy ϵ of the terms L_S, L_a, and $T_{\bar{45}}$ against the pressure p for $Bi_{1-x}Sb_x$ alloys: a—$x < 0.04$, b—$0.06\,(5) > x > 0.04$.

3. DISCUSSION OF RESULTS

1. The foregoing results indicate that the scheme proposed in[8] for the motion of the terms L_S and L_a under pressure is valid for $Bi_{1-x}Sb_x$ alloys with $x < 0.04$ and $x > 0.04$ (see Fig. 1b in[8]).

The scheme of simultaneous motion of the terms L_S and L_a as well as the top of the valence band at the point T (the term $T_{\bar{45}}$[8]) as a function of the pressure for these two cases is shown in Fig. 9. The coming together and reflection of the terms L_S and L_a under pressure for alloys with $x > 0.04$ explains the presence of a maximum on the S(p) curves for the electron and hole sections. The pressure $p = p_m$ corresponds to the minimum distance between terms L_S and L_a, while $p = p_{cr}$ corresponds to the intersection of the terms L_S and $T_{\bar{45}}$.

The observed experimental increase of p_m with increasing Sb concentration is connected with the increase of the gap ϵ_g at $x > 0.04$[7], and agrees with the assumption that $\partial\epsilon_g/\partial p$ is constant (at $p < p_m$) for different Sb concentrations.

On the other hand, p_{cr}, which corresponds to the lifting of the overlap in the alloy, decreases with increasing Sb concentration for both types of alloys, for in this case the initial overlap of the terms L and T is decreased.

Near the inversion point of the terms L_S and L_a, both under the influence of the Sb impurity (at $x \sim 0.04$) and under the influence of pressure (at $p \approx p_m$ for the alloys with $x > 0.04$), a sharp decrease takes place in the effective masses of the electrons at the bottom of the conduction band[7,8]. However, the overlap of the bands at the points L and T causes only relatively small changes of the masses and electron mobilities to be observed at the Fermi level. The situation changes at Sb concentrations such that the term $T_{\bar{45}}$ (at atmospheric pressure) lies lower than the center of the gap ϵ_g. In this case there is no overlap when the terms L_S and L_a come closer together under the influence of the pressure, and the effective carrier masses become anomalously small[8].

The term T^- drops with increasing pressure relative to the center of the gap ϵ_g. Favoring this is the fact that for any Sb concentration the cyclotron masses of the electrons m^e decrease upon compression. The absolute values of the term velocities under the influence of the pressure, on the basis of the experimental dependences of S^e, S^h, and m^e on p, can be obtained only by using the concrete model of the electron spectrum, which makes it possible to calculate the Fermi energies of the electrons and holes, ϵ^e_F and ϵ^h_F, and the overlap energy ϵ_{0V}.

The present data, as well as those of[7,17,18], indicate that the electron dispersion in $Bi_{1-x}Sb_x$ alloys is satisfactorily described by the model of an ellipsoidal nonparabolic spectrum (the Lax ENP model[19]), supplemented with the dependence given by Golin[6] for the effective mass at the bottom of the conduction band m^e_0 on the energy gap ϵ_g.

The extremal sections of the electron ellipsoid S^e and the cyclotron masses m^e at the Fermi level are connected in this model with m^e_0 at the bottom of the band and the parameters of the spectrum ϵ^e_F and ϵ_g by the following relations:

$$S^e = 2\pi m_0^e \varepsilon_F^e (1 + \varepsilon_F^e/\varepsilon_g), \tag{1}$$

$$m^e = m_0^e (1 + 2\varepsilon_F^e/\varepsilon_g), \tag{2}$$

$$m_0^e = \gamma\varepsilon_g. \tag{3}$$

Like m^e_0, the coefficient γ depends on the direction of the magnetic field relative to the crystal axes, but, according to[7], it does not depend on the Sb concentration. In the reduction of the experimental data within the framework of the chosen model, it is assumed that γ is independent of the pressure. For all the Sb concentrations and for all pressures, we used the values of γ calculated on the basis of the data of[15,16] for Bi. In particular, at $H \parallel C_2$ we have $\gamma C_2 = 1.38 \times 10^{-4}\, m_0\,[\text{meV}^{-1}]$.

Equations (1)—(3) can be solved relative to ϵ^e_F, ϵ_g, and m^e:

$$\varepsilon_F^e = \frac{m^e}{2\gamma} - \left[\left(\frac{m^e}{2\gamma}\right)^2 - \frac{S^e}{2\pi\gamma}\right]^{1/2} \quad (4)$$

$$\varepsilon_g = 2\left[\left(\frac{m^e}{2\gamma}\right)^2 - \frac{S^e}{2\pi\gamma}\right]^{1/2}, \quad (5)$$

$$m^e = 2\gamma\left[\left(\frac{\varepsilon_g}{2}\right)^2 + \frac{S^e}{2\pi\gamma}\right]^{1/2}. \quad (6)$$

Relations (4) and (5) make it possible to calculate ϵ_F^e and ϵ_g from the experimentally measured m^e and S^e.

To calculate the hole Fermi energy ϵ_F^h we used the relation

$$\varepsilon_F^h = S^h/2\pi m^h, \quad (7)$$

which is valid for a quadratic dispersion law.

The concentration dependences of the quantities ϵ_F^e, ϵ_F^h, ϵ_g and $\epsilon_{ov} = \epsilon_F^e$ plus ϵ_F^h, calculated in accordance with formulas (4), (5), and (7), are shown in Fig. 10a. Figure 10b shows the scheme, corresponding to Fig. 10a, of the motion of the terms L_S, L_a, and $T_{\overline{45}}$ under the influence of the impurity Sb. The same figure shows the points from [7,15-18]. It is seen from Fig. 10a that the results of the calculation of ϵ_g are in good agreement with the concept of band inversion at L when $x \sim 0.04$.

It is of interest to compare data obtained by different workers on the electron sections in $Bi_{1-x}Sb_x$ alloys with different Sb concentrations with the present results. The generalized plot of the ratio of the extremal electron sections to the corresponding sections of Bi is shown in Fig. 11. Extrapolation of $S^e(x)$ to zero yields an Sb concentration of approximately 0.06 (5) for the point where the overlap is lifted.

It should be noted that the present data on S^e and m^e form, within the framework of the Lax-Golin model (formulas (1)–(3)), a closed system with the data of

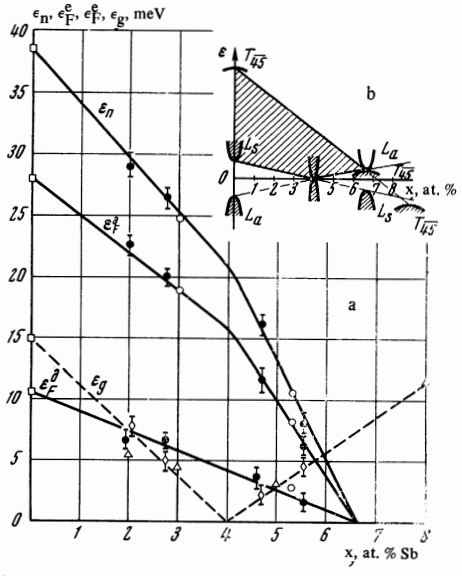

FIG. 10. a–Dependence of the overlap energy ϵ_{ov}, the Fermi energies ϵ_F^e and ϵ_F^h of the electrons and holes, and the energy gap ϵ_g on the Sb concentration: ● and ◇–present data, □–[15,16], △–[7], ○–[17,18]; b–qualitative form of the dependence of the energy ϵ of the terms L_S, L_a, and $T_{\overline{45}}$ on the Sb concentration in $Bi_{1-x}Sb_x$ alloys.

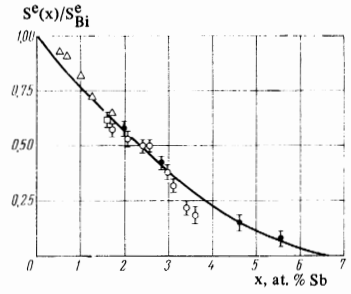

FIG. 11. Dependence of the ratio of the extremal electron section of $Bi_{1-x}Sb_x$ alloys to the corresponding cross section of Bi on the Sb concentration: ●–present data, △–[22], □–[23], ○–[24].

Table I.

Parameter	$\partial\epsilon/\partial p$, 10^{-6} eV/bar		
	$0 < x < 0.04$	$0.04 < x < 0.065$	
		$p < p_m$	$p > p_m$
$\partial\varepsilon_h/\partial p$	~ -1.4	$\sim +0.4$	~ -1.3
$\partial\varepsilon_g/\partial p$	$\sim +1.0$	~ -2.4	$\sim +1.0$

Table II.

	$\partial\epsilon/\partial x$, 10^{-3} eV/at. % (p = 1 bar)	
	$0 < x < 0.04$	$0.04 < x < 0.065$
$\partial\epsilon_F^e/\partial x$	~ -2.9	~ -6.2
$\partial\epsilon_F^h/\partial x$	~ -1.7	~ -1.7
$\partial\varepsilon_p/\partial x$	~ -4.5	~ -7.9
$\partial\varepsilon_g/\partial x$	~ -3.8	$\sim +2.9$

Tichovolsky and Mavroides[7] on ϵ_g and m_0^e. On the other hand, on the basis of the dependence of S^e (Fig. 11) and of ϵ_g on x (Fig. 7, curve B), see (3)), we can calculate the dependence of m^e on x from (6). This is shown by the solid line of Fig. 7 (curve A). We see that the experimental points for m^e fit this curve quite well. On the other hand, the points obtained for ϵ_g by means of formula (5) on the basis of data for m^e and S^e are in sufficiently good agreement with the data of[7] (Fig. 10a).

A numerical calculation of the quantities ϵ_g, ϵ_F^e, ϵ_F^h, and $\epsilon_{ov} = \epsilon_F^e + \epsilon_F^h$ by means of formulas (4), (5), and (7) at different Sb concentrations and at different pressures makes it possible to estimate the rates of their variation under these types of action on the Bi spectrum. It was assumed for the estimates that in the first approximation the displacement of the terms L_S, L_a, and $T_{\overline{45}}$ is linear in p and x (as is shown qualitatively in Figs. 9a, 9b, and 10b), with the exception of the inversion points, where the rates of displacement experience jumps. The results of the estimates are given in Tables I and II.

2. Let us analyze the dependence of m^e on the Sb concentration and on the pressure. From (2) and (3) it follows that

$$m^e = 2\gamma(\varepsilon_F^e + {}^1/_2\varepsilon_g), \quad (8)$$

whence

$$\partial m^e/\partial x = 2\gamma(\partial\varepsilon_F^e/\partial x + {}^1/_2\partial\varepsilon_g/\partial x), \quad (9)$$

$$\partial m^e/\partial p = 2\gamma(\partial\varepsilon_F^e/\partial p + {}^1/_2\partial\varepsilon_g/\partial p). \quad (10)$$

Expression (8) shows that the change of m^e is determined by the quantity $E_F = \epsilon_F^e + (1/2)\epsilon_g$, which represents the Fermi energy reckoned from the center of the energy gap ϵ_g. A nearly-linear decrease of m^e in the Sb concentration interval from 0 to ~0.06 (5) points to an analogous variation of E_F from the value $\epsilon_F^e + (1/2)\epsilon_g$ for Bi to $(1/2)\epsilon_g$ at $x \approx 0.06$ (5). Such a change of E_F indicates that the rate of downward motion of the term T^- under the influence of the Sb impurity is much larger than the rate of relative motion of the terms L_a and L_s. The weak decrease of m^e with pressure indicates, on the other hand, that the rates of motions of the terms T^-, L_a, and L_s are in this case close to each other, and the influence of their motion on E_F is practically cancelled out mutually (the first and second terms of (10) have opposite signs).

One could expect that with increasing pressure, the weak decrease of m^e would give way to an increase, if it were assumed that the linear growth of ϵ_g would continue in this region of pressures. The expected character of the $m^e(p)$ dependence is illustrated in Fig. 8. The solid curve in this figure was calculated from formula (6) for the alloy $Bi_{0.9725}$, $Sb_{0.0275}$ on the basis of the measured S^e (Fig. 2, curve B) and the relation

$$\varepsilon_g(p) \approx \varepsilon_g(0) + 1.0 \cdot 10^{-6}\ (\text{eV/bar})\ (\text{bar})$$

which is valid for alloys with $x < 0.04$ and $x > 0.04$ at $p > p_m$.

We see that the weak decrease of m^e first gives way to an increase at $p > 10$ kbar. Unfortunately, in the region $p > 10$ kbar it was impossible to observe oscillations of the longitudinal magnetoresistance with a clarity sufficient to determine m^e. At $p < 10$ kbar, the experimental values of m^e agree with the curve of Fig. 8 within the limits of the measurement errors.

3. The relation $H_m(p)/H_m(0) \approx S^e(p)/S^e(0)$ at $p < p_{cr}$, indicates for each type of alloy that there is a connection between the field H_m at the maximum of the non-oscillating part of $\rho(H)$ and the parameters of the energy spectrum. A determination of this connection not only can yield additional information on the spectrum, but may also be useful for an elucidation of its variation under pressure in conditions when the oscillation effects cannot be observed (insufficiently pure samples, small band overlaps, the presence of a thermal gap in the alloy, etc.).

Since the carrier mobility decreases in a magnetic field, the maximum of $\rho(H)$ can be observed only on a rearrangement of the spectrum in the field such that the carrier density increases sufficiently rapidly.

The electron and hole densities n and p can be increased in the magnetic field by two mechanisms. The first consists of an increase of the overlap or a decrease of the forbidden band (at $T \neq 0°K$) upon displacement of the band boundaries[2,20,21]. For the semimetallic $Bi_{1-x}Sb_x$ alloys whose energy spectrum is shown schematically in Fig. 1, at certain orientations of the magnetic field (for example, at $H \parallel C_2$), the following inequality may be satisfied[12,13,15]

$$\alpha = \frac{e\hbar}{c}\left(\frac{1}{m_s^e} - \frac{1}{m^e} + \frac{1}{m_s^h} - \frac{1}{m^h}\right) > 0,$$

where m_s^e and m_s^h are the spin masses of the electrons and holes, e the electron charge, c the velocity of light, $\hbar = h/2\pi$, and h is Planck's constant. In this case the overlap in the field increases linearly:

$$\varepsilon_h(H) = \varepsilon_{h_0} + \alpha H,$$

where $\epsilon_0 v_0$ is the overlap energy at $H = 0$. The parameter α can be estimated from the data of Smith, Baraff, and Rowell[15]. At $H \parallel C_2$ we obtain for Bi the value $\alpha \approx 0.17$ meV/kOe.

The second mechanism whereby the carrier density is changed in a field is connected with the change of the electron and hole Fermi energies when their cyclotron masses are appreciably different ($m^e \ll m^h$). In this case the ultraquantum limit for light carriers is reached in much weaker fields than for heavy ones. After emergence of the 0^+ level of the electrons at $H = H_{0+}^e$, the degeneracy of the last level 0^- begins to increase rapidly. This is accompanied by a decrease of ϵ_F^e and an increase of ϵ_F^h practically to a value equal to ϵ_{0v} (all the carriers contained within the band-overlap region condense on the 0^- level). During the course of this process, the carrier density $n = p$ increases and then remains practically constant until the emergence of the 0^+ level of the holes at $H = H_{0+}^h$, after which the concentration $n = p$ first decreases, and then increases linearly in the field, in proportion to the degree of the degeneracy of the 0^- levels of the electrons and holes. The second mechanism leads to a local increase of the carrier density in a relatively narrow field region at $H > H_{0+}^e$.

To estimate the contribution of the second mechanism, we present a quantitative analysis of the relation $n(H) = p(H)$, neglecting the deviation of the electron dispersion from quadratic. It can be shown that allowance for the non-quadratic dispersion does not change the calculation results significantly. In order to describe the second mechanism independently of the first, we put in the calculation $m_s^e = m^e$, $m_s^h = m^h$, and $\alpha = 0$. This means that the overlap does not change in the field, and the 0^- levels of the electrons and holes are located respectively at the bottom of the conduction band at L and at the top of the valence band at T (the band boundaries are fixed).

The electron (or hole) state density $g(\epsilon)$ in the magnetic field[15] is equal to

$$g(\varepsilon) = 2^{3/2}\frac{eH}{ch^2}\frac{(m_c^e)^{3/2}}{m^e}\sum_{n=0,\ s=\pm 1}^{n_{max}}\frac{1}{2}\cdot\left[\varepsilon - \left(n+\frac{1}{2}\right)\frac{e\hbar H}{m^e c} - \frac{1}{2}s\frac{e\hbar H}{m_s^e c}\right]^{-1/2}, \tag{11}$$

where m_c^e is the state-density mass, and the summation extends over all integer n for which the radicand is larger than zero.

In the case of complete degeneracy, the non-oscillating part of the electron and hole density is determined at different values of the magnetic fields by the following relations:

a) In the case $H < H_{0+}^e$

$$n = p \approx \frac{8\pi}{3}\left[\frac{2}{h^2}\frac{m_c^e m_c^h}{m_c^e + m_c^h}\varepsilon_h\right]^{3/2}; \tag{12}$$

b) in the case $H_{0+}^e < H < H_{0+}^h$

$$n = 2^{3/2}\frac{eH}{ch^2}\frac{(m_c^e)^{3/2}}{m^e}(\varepsilon_F^e)^{1/2}, \qquad p \approx \frac{8\pi}{3}\left[\frac{2}{h^2}m_c^h\varepsilon_F^h\right]^{3/2},$$

$$n = p,\ \varepsilon_F^e + \varepsilon_F^h = \varepsilon_h; \tag{13}$$

c) in the case $H > H_{0+}^h$

$$n = 2^{3/2}\frac{eH}{ch^2}\frac{(m_c^e)^{3/2}}{m^e}(\varepsilon_F^e)^{1/2}, \tag{14}$$

$$p = 2^{3/2}\frac{eH}{ch^2}\frac{(m_c^h)^{3/2}}{m^h}(\varepsilon_F^h)^{1/2},$$

$$n = p,\ \varepsilon_F^e + \varepsilon_F^h = \varepsilon_h.$$

Equations (12)–(14) cannot describe the dependence of the carrier density n = p on the field in the regions $H \sim H_+^e$ and $H \sim H_{0+}^h$, where allowance for several terms in the sum of (11) is important.

The qualitative form of the dependence of n = p on H is shown by curve a of Fig. 12. In region I, formula (12) is valid.

When $H > H_{0+}^e$ ($H_{0+}^e \approx m^e c\epsilon_F^e/e\hbar$), the dependence of n = p on H in region II ($4a^2H^2/27\epsilon_{0V}^2 \ll 1$, where $a = (3/4)(m_c^e/m_c^h)^{3/2}e\hbar/m^e c$) is described by the formula

$$n_{II} = p_{II} \approx \frac{8\pi}{3}\left(\frac{2m_c^h}{h^2}\right)^{3/2} aH\varepsilon_h^{1/2}. \tag{15}$$

For the $Bi_{1-x}Sb_x$ alloys (at $H \parallel C_2$), region II is contained between H_{0+}^e and $(2-3)H_{0+}^e$.

Beyond this, the growth of the concentration exhibits saturation (region III).

In region IV we have

$$n_{IV} = p_{IV} \approx \frac{8\pi}{3}\left(\frac{2m_c^h}{h^2}\varepsilon_h\right)^{3/2}. \tag{16}$$

The ratio $n_{IV}/n_I = ((m_c^e + m_c^h)/m_c^e)^{3/2} \approx 8-12$ for the $Bi_{1-x}Sb_x$ alloys.

In region V, at $H > H_{0+}^h$ ($H_{0+}^h \approx m^h c\epsilon_{0V}/e\hbar$), the concentration decreases by a factor $\sim (4/3)(1 + m_Z^h/m_Z^e)^{1/2} \approx (3-7)$, where $m_Z^e = (m_c^e)^3/(m^e)^2$; $m_Z^h = (m_c^h)^3/(m^h)^2$.

In region VI, the concentration increases linearly in accordance with the formula

$$n_{VI} = p_{VI} = 2^{3/2}\frac{eH}{ch^2}\left(\frac{1}{m_z^e} + \frac{1}{m_z^h}\right)^{-1/2}\varepsilon_h^{1/2}, \tag{17}$$

which coincides with the analogous expression in[25].

The qualitative form of the dependence of n = p on H under simultaneous action of the first and second mechanisms is shown in Fig. 12 by curve b. Since now $\alpha > 0$, formulas (12) and (15)–(17) must be modified in the following manner: in (12) we replace ϵ_{0V} by $\epsilon_{0V0} + \alpha H$; we replace ϵ_{0V} in (15) and (17) by $\epsilon_{0V0} + 2\alpha H$, and (16) takes the form

$$n_{IV} = p_{IV} \approx \frac{8\pi}{3}\left(\frac{2m_c^h}{h^2}\right)^{3/2} aH(\varepsilon_{h0} + 2\alpha H)^{1/2}Q, \tag{18}$$

where ϵ_{0V0} is the overlap energy in the absence of a field.

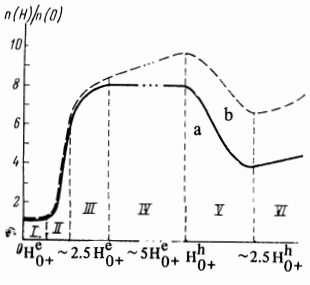

FIG. 12. Qualitative form of the relative change of the carrier density in a magnetic field for $Bi_{1-x}Sb_x$ alloys with $x < 0.06$ (5): a–band boundaries fixed ($\alpha = 0$); b–the overlap increases linearly in the field ($\alpha > 0$)

$$Q = 2^{-1/2}\left\{\left[1 + \left(1 + \frac{a^2}{27\alpha^2}\right)^{1/2}\right]^{1/3} + \left[1 - \left(1 + \frac{a^2}{27\alpha^2}\right)^{1/2}\right]^{1/3}\right\}^{3/2}.$$

Following this change, formula (17) coincides also with the corresponding expression in[25].

It is seen from Fig. 12 that the fastest growth of the concentration occurs in region II at $H_{0+}^h < H < (2-3)H_{0+}^e$. The values of H_m for the $Bi_{1-x}Sb_x$ alloys lie in the same field interval. It is therefore natural to connect the formation of the maximum of $\rho(H)$ with region II. Since it is sufficiently narrow, the approximate relation $H_m \approx kH_+$ is satisfied, where $k \sim (2-3)$. In turn, H_{0+}^e is proportional to S^e, from which it follows that

$$H_m(p)/H_m(0) \approx S^e(p)/S^e(0).$$

For an analytic calculation of H_m it is necessary to know the dependence of the electron and hole mobilities μ and ν on the field. A rought estimate can be obtained by assuming that $\nu \ll \mu$ and that μ depends on H like $1/H\beta$. In this case we can show for $\alpha > 0$, on the basis of (15), that the minimum of the conductivity σ in region II is observed at H_m proportional to ϵ_{0V0}/α, if $1.0 < \beta < 1.5$. This likewise agrees qualitatively with the relation $H_m \propto S^e$.

We note that the quantum limit for the holes at $\alpha > 0$ and $e\hbar/m^h c < \alpha$ can be reached for the quantum numbers of the Landau levels with $n > 0$. (Both inequalities are apparently valid for the $Bi_{1-x}Sb_x$ alloys at $H \parallel C_2$). In this case, the following relations are satisfied for a certain value of n:

$$\left(n + 1 + \frac{1}{2}\right)\frac{e\hbar}{m^h c} > \alpha, \quad \left(n + \frac{1}{2}\right)\frac{e\hbar}{m^h c} < \alpha,$$

which mean that the Fermi level, owing to the growth of the overlap in the field, overtakes all the Landau levels with numbers smaller than n + 1. The last minimum of the hole oscillation corresponds in this case to the emergence of the (n + 1)-st level. The levels with the smaller quantum numbers do not take part in the oscillations. This circumstance must be borne in mind when the quantum numbers corresponding to the minima of the hole oscillations are determined. When $e\hbar/m^h c < \alpha$, the character of the dependence of the concentration on H can also change noticeably in regions V and VI (Fig. 12).

For the $Bi_{1-x}Sb_x$ alloys in the semiconducting state (at a pressure $p > p_{cr}$), the maximum of $\rho(H)$ ($H \parallel C_2$) can be the result of the decrease of the gap ϵ_g in the magnetic field; in the first approximation, this decrease is linear[20]. It can be shown in this case that $H_m \propto \Delta E_T/k_B T$, under the assumption that $\mu \gg \nu$ and $\mu \propto 1/H\beta$ (ΔE_T is the thermal gap, and k_B is Boltzmann's constant) for all values $\beta > 0$.

In conclusion, we take the opportunity to thank E. A. Svistova and Ya. G. Ponomarev for useful discussions, and É. Ioon for help with the data reduction.

[1] I. M. Lifshitz, Zh. Eksp. Teor. Fiz. 38, 1569 (1960) [Sov. Phys.-JETP 11, 1130 (1960)].

[2] M. Ya. Azbel' and N. B. Brandt, ibid. 48, 1206 (1965) [21, 804 (1965)].

[3]N. B. Brandt and Ya. G. Ponomarev, Zh. Eksp. Teor. Fiz. 55, 1215 (1968) [Sov. Phys.-JETP 28, 635 (1969)].
[4]L. S. Lerner, Phys. Rev., 127, 1480 (1962).
[5]N. B. Brandt, PTE No. 2, 138 (1956).
[6]S. Golin, Phys. Rev. 176, 830 (1968).
[7]E. J. Tichovolsky and J. G. Mavroides, Solid State Comm., 7, 927 (1969).
[8]N. B. Brandt, H. Dittmann, Ya. G. Ponomarev, and S. M. Chudinov, ZhETF Pis. Red. 11, 250 (1970) [JETP Let. 11, 160 (1970).
[9]N. B. Brandt and N. Ya. Minina, ibid. 7, 264 (1968) [7, 205 (1968)].
[10]E. S. Itskevich and L. M. Fisher, Zh. Eksp. Teor. Fiz. 53, 98 (1967) [Sov. Phys.-JETP 26, 66 (1968)].
[11]E. S. Itskevich, I. P. Krechetova and L. M. Fisher, ibid. 52, 66 (1967) [25, 41 (1967)].
[12]N. B. Brandt, E. A. Svistova, Yu. G. Kashirskiĭ, and L. V. Lyn'ko, ibid. 56, 65 (1969) [29, 35 (1969)].
[13]N. B. Brandt, E. A. Svistova, and R. G. Valeev, ibid. 55, 469 (1968) [28, 245 (1969)].
[14]E. Adams and T. Holstein, J. Phys. Chem. Soc., 10, 254 (1959).
[15]G. E. Smith, G. A. Baraff, and J. M. Rowell, Phys. Rev., 135, A1118 (1964).
[16]R. T. Isaakson and G. A. Williams, Phys. Rev., 185, 682 (1969).
[17]L. Wehrli, Phys. Kondens, Materie, 8, 87 (1968).
[18]M. R. Ellett, R. B. Horst, L. R. Williams, and K. F. Cuff, J. Phys. Soc. Japan, Suppl., 21, 666 (1966).
[19]B. Lax, J. G. Mavroides, Il. J. Zeiger, and R. T. Keyes, Phys. Rev. Lett., 5, 241 (1960).
[20]G. A. Baraff, Phys. Rev., 137, A842 (1965).
[21]N. B. Brandt, E. A. Svistova, and Yu. G. Kashirskiĭ, ZhETF Pis. Red. 9, 232 (1969) [JETP Let. 9, 136 (1969)].
[22]N. B. Brandt and V. V. Shchekochikhina, Zh. Eksp. Teor. Fiz. 41, 1412 (1961) [Sov. Phys.-JETP 14, 1008 (1962)].
[23]J. H. Kao, D. R. Brown, and R. L. Hartmann, Phys. Rev., 136, A858 (1964).
[24]L. G. Lyubutina, Candidate's Dissertation, Moscow State University, 1967.
[25]A. A. Abrikosov, Zh. Eksp. Teor. Fiz. 56, 1391 (1969) [Sov. Phys.-JETP 29, 746 (1969)].

Translated by J. G. Adashko
172